

## 4. On the Issue of Urea Phase Connectivity in Formulations Based on Molded Flexible Polyurethane Foams

### 4.1 Chapter Summary

Lithium chloride was added to systematically alter the phase separation behavior, and hence the nature of urea phase connectivity, in a series of plaques based on molded flexible polyurethane foam formulations. The plaques prepared were found to possess varied levels of urea phase connectivity which was examined at different length-scales using several characterization techniques. SAXS, TEM, and *t*-AFM were used to show that addition of LiCl systematically reduced the formation of the urea aggregate structures typically observed in flexible polyurethane foam formulations and thus led to a loss in urea phase connectivity at the *macro* level. SAXS, DSC, and DMA revealed that formulations with and without LiCl exhibited similar interdomain spacings and soft segment glass transitions, suggesting that incorporation of LiCl did not prevent the plaques from undergoing partial microphase separation. WAXS demonstrated that addition of LiCl led to a loss in the local ordering of the hard segments within the microdomains, i.e., it led to a reduction of *micro* level connectivity or the regularity in segmental packing of the urea phase. High magnification *t*-AFM images showed that increasing the LiCl content dispersed the urea component more homogeneously and in a more uniform manner in the polyol matrix, and thus altered the connectivity of the urea phase at the microdomain level.

### 4.2 Introduction

Polyurethanes<sup>1</sup> are used in a wide range of applications including foams, fibers, elastomers, coatings, and adhesives. This makes polyurethanes an important class of materials with high production quantities. For instance, the 2000 urethanes market is estimated to be of the order of 8.2 million metric tons worldwide.<sup>2</sup> Amongst the above mentioned applications, flexible polyurethane foams<sup>3</sup> take up a large portion of the market share and are used in furniture, packaging, thermal insulation, and transportation based applications. Depending on the desired end use, flexible polyurethane foams are commonly made by either a slabstock or a carousel molded technique – the slabstock process being continuous while the molded process is of a semi-continuous nature.

The chemistry involved in the production of flexible polyurethane foams is based on two well understood reactions. In the first reaction, called the ‘blow’ reaction, water reacts with an isocyanate group to yield an amine functionality, carbon dioxide, and heat. The amine group formed further reacts with another isocyanate group to yield a urea linkage. The evolved gas and the reaction exotherm help to open and develop the already nucleated bubbles in the reacting mixture into foam cells. Due to a simultaneously occurring reaction, in which an isocyanate group reacts with a hydroxyl functionality (from a polyol with  $f > 2$ ) to yield a urethane linkage, this expanding mixture ‘gels’ and gives the foam a stable open-celled cellular structure. The above reaction scheme results in the solid portion of the foam possessing a phase separated morphology consisting of a harder urea phase (as a result of the blow reaction), which is covalently bonded to the softer polyol phase through urethane linkages (which arise due to the gelation reaction).

It needs to be mentioned, that in the present study, ‘plaques’ based on molded flexible foam formulations have been investigated. The ‘plaque’ formulations differ from actual ‘foam’ recipes in that they do not incorporate a surfactant, since addition of a surfactant is *not* critical in the formation of a plaque (as there is no desire to stabilize the cellular structure). The influence of a surfactant on the solid-state morphology of slabstock flexible polyurethane foams was recently investigated by Kaushiva et. al.<sup>4</sup> In that study, workers observed that foams with and without surfactant exhibited dissimilarities in the urea aggregation behavior. However, in the past, it has also been observed that the *trends observed in the morphological features of plaques strongly resemble those of actual foams with similar compositions*,<sup>5,6</sup> which rationalizes the present investigation of ‘plaques’ as a means of indirectly studying foam morphology. Thus, the key results obtained from this study will be expected to be similar for actual flexible foam materials, and this issue will be discussed in greater detail in Chapter 6.

The isocyanate commonly employed in flexible polyurethane foam production is an 80:20 blend of 2,4/2,6 toluene diisocyanate (TDI), but other blends and other isocyanates are also sometimes utilized. The isocyanate moieties, through successively reacting with water molecules on each end, result in linear polyurea ‘hard’ segments. When the concentration of these hard segments generated exceeds a system-dependent solubility limit, the hard segments precipitate out and form what are commonly referred to as urea microdomains. These urea microdomains act as physical or pseudo cross-linking points and enhance their cohesive strength

from bidentate hydrogen bonding. The polyols used have average functionalities in the range of 2.5-3, and thus provide covalent cross-linking points.

In addition, at higher water contents (and thus at higher hard segment contents), the urea microdomains are known to aggregate and form larger urea rich structures commonly termed as ‘urea balls’ or ‘urea aggregates’.<sup>3,5</sup> Workers have observed, using x-ray microscopy, that these aggregate phases are not completely isolated from the surrounding matrix, but have some polyol residing in them.<sup>7</sup> Also, these urea balls are observed to be bigger in size and more easily observed in conventional slabstock formulations as compared to molded or high-resiliency (HR) foams of the same water content. This difference arises due to the difference in the chemistry of the constituents which make up the formulations. While both slabstock and molded (HR) foams utilize the commonly used 80:20 2,4/2,6 TDI blend, the polyols used in each type of foam differ considerably. The polyol molecular weight is typically higher in molded foams as compared to slabstock foams (ca. 5000 g/mol for molded polyols and ca. 3000 g/mol for slabstock polyols) to achieve faster viscosity build-up during the gelation reaction and thus resulting in shorter demold times. In addition, molded polyols are usually end-capped with ethylene oxide (EO) to enhance the reaction rate. End-capping with EO also promotes mixing of the water and the polyol phases. Finally, a copolymer polyol (CPP), which acts as a filler particle is sometimes added in molded formulations to improve load-bearing properties of the foam. The influence of CPP on the structure-property relationships of molded flexible foams has been discussed in reference 8.

Molded foam formulations also differ from slabstock formulations in that they often utilize a cross-linking agent. The commonly used cross-linking agent is diethanol amine (DEOA) and is added at levels of ca. 1.0-2.0 parts per hundred polyol (pphp). This additive facilitates the foam to achieve dimensional stability faster and thus helps in attaining shorter demold times. Kaushiva and Wilkes studied the effect of DEOA on morphology and found that DEOA had a disrupting effect on the bidentate hydrogen bonding within the microdomains of the polymer.<sup>9</sup> Their work suggested that DEOA primarily resides in the microdomains and reduces the extent of local ordering and thus the regularity in segmental packing of the microdomains. In addition, they observed, using AFM and SAXS, that incorporation of DEOA led to the formation of microdomains ca. 5 nm in size, in comparison to the foam without DEOA in which the microdomains were present, but often aggregated and formed ca. 50 nm size structures.<sup>9,10</sup> These observed changes in the morphology were also correlated to the physical properties of the foam.

Foams containing DEOA were found to have lower rubbery moduli and lower load-bearing properties. Their work thus suggested that a loss in the physical associations of the urea phase on addition of DEOA resulted in a significant softening of the foams – thus implying that a change in the connectivity of the urea phase played an important role in determining the physical properties of the foam.

Besides the issues of connectivity or the packing regularity of the hard segments, and the connectivity of the urea hard phase at the microdomain level, also of importance is the urea aggregate connectivity. This chapter attempts to characterize the different levels of urea phase connectivity which are present in flexible foam formulations in general, and *molded* flexible foam formulations in particular. While WAXS is used to probe connectivity or the nature of packing of the hard segments at the *micro* level, other suitable characterization techniques are applied to examine connectivity at greater length-scales. Transmission electron microscopy in conjunction with SAXS is used to assess the presence of the urea aggregates and can thus give insight into *macro*-connectivity levels. AFM has the capability to image features at the microdomain level and can thus give valuable information on microdomain connectivity, as will be discussed later in this chapter.

The choice of using lithium chloride as an additive in flexible polyurethane foams extends from the work of Moreland et. al., where they attempted to produce ‘softer’ foams which utilized no physical blowing agents and yet maintained high water contents.<sup>11</sup> These workers investigated a series of foams with 0.0, 0.4 and 0.5 LiCl pphp, while maintaining the hard segment content constant. They observed via TEM that there was a reduction in the formation of urea rich aggregates in foams containing LiCl. SAXS experiments carried out as a part of the same study suggested that systems with and without LiCl were microphase separated and possessed similar interdomain spacings. It was also observed via WAXS that the local ordering of the hard segments within the microdomains was lost on addition of LiCl. Their work suggested that LiCl acted as a localized “hard-segment plasticizer” and thus resulted in foams with lower moduli. However, at that point, addressing the issue of urea phase connectivity and its influences on foam properties was not an objective of their investigation. In contrast, the focus of the present study has been to characterize urea phase connectivity using LiCl as a probe, and thus a broader range of LiCl containing formulations, from 0.0 to 1.5 LiCl pphp have been utilized.

Interactions between polar groups of polymers with metallic ions provide opportunities to alter the structure of the polymer in various aspects. The presence of LiCl is known to disrupt hydrogen bonding effects which might be present in a polymer. For this reason, LiCl as well as some other lithium salts are commonly utilized for dissolution of polymer samples in order to determine the molecular weight distribution (MWD) using gel permeation chromatography. For example, lithium chloride has been used in the measurement of the MWD of Kevlar.<sup>12</sup> Workers have also investigated the interaction of lithium cations with polyurethane elastomers and their effect on the overall bulk conductivity of the polymer.<sup>13,14</sup> In the current class of materials investigated, the presence of LiCl in the reacting mixture has two major effects. Firstly, it alters the solubilization features of the added co-reactants, which are known to exist in different phases. Secondly, it slows down the blow reaction by partially blocking the amine catalyst, and thus alters the reaction kinetics involved. Thus, the addition of LiCl presents an opportunity to study polyurethane foam formulations with different phase separation characteristics, and hence examine the different levels of urea phase connectivity which might be present.

In light of the above discussion, it is clear that polyurethane foams can possess vastly different morphologies with different levels of urea phase connectivity. Thus it is of interest to understand the urea phase connectivity as it undoubtedly strongly influences the physical properties of the polymer. Urea phase connectivity levels can be altered by several methods. As discussed previously, incorporation of DEOA alters the urea aggregation behavior and also leads to differences in connectivity at the hard segment level. Another way to alter urea phase connectivity would be by switching from a slabstock polyol to a molded polyol since the nature of the polyol is known to have an influence on the urea aggregation characteristics. Altering the ratio of the isocyanates (2,4:2,6 TDI ratio) would lead to different hard segment packing characteristics due to symmetry arguments and also possibly lead to different kinds of urea aggregation behavior. Changing the hard segment content by controlling the water content would also undoubtedly alter urea phase connectivity based on volume fraction arguments. However, it is important to note that though all the above routes can be utilized to change urea phase connectivity, each case mentioned above leads to an alteration in the final covalent polymeric network. Lithium chloride, on the other hand, does not covalently react into the polymer network, and yet leads to networks which possess different urea phase connectivity by changing the solubilization characteristics of the different phases involved, as well as by altering the

reaction kinetics. Finally, the author would like to restate that the present study will focus *only* on understanding urea phase connectivity in *molded* flexible polyurethane foams using a variety of characterization techniques. A detailed investigation on the influence of urea phase connectivity on the physical properties of the polymer has already been discussed in Chapter 3.

## 4.3 Experimental

### 4.3.1 Materials

A series of plaques based on Voranol 4703<sup>®</sup> were prepared at The Dow Chemical Company in Freeport, Texas. Voranol 4703<sup>®</sup> is a commercial grade polyol produced by Dow Chemical with an equivalent weight of 1667 and an average functionality of 2.50. This EO-capped polyol is primarily used in molded flexible polyurethane formulations and has an EO content of 16%. All formulations were based on a TDI index of 100 and a 4.5 parts per hundred polyol (pphp) water content. The catalyst package, which was used at a level of 0.2 pphp, consisted of 5 parts by weight of Dabco 33LV for each part of Dabco BL11. Specific details regarding the catalysts can be found elsewhere.<sup>3</sup> The LiCl content was varied in a systematic manner to obtain samples with varied levels of urea connectivity. As stated earlier, a broader range of LiCl content is studied in this chapter as compared to the study carried out by Moreland et. al.<sup>11</sup> Six formulations were prepared containing 0.0, 0.1, 0.2, 0.5, 1.0 and 1.5 LiCl pphp. Though these concentrations of LiCl might appear relatively small, they are not. This is due to the fact that LiCl is a low molecular weight species. For example, in the 1.5 LiCl pphp formulation, there exist ca. 1.45 LiCl molecules for every soft segment (polyol) molecule. Simple calculations also show that, for every isocyanate and water molecule present in the 1.5 LiCl pphp formulation, there are present ca. 0.13 and 0.14 LiCl molecules respectively. It is also mentioned that for 100 g of polyol, the molar quantities of the polyol, isocyanate, and water are 0.024, 0.280, and 0.25 moles respectively. The 0.0, 0.1, 0.2, 0.5, 1.0 and 1.5 LiCl pphp correspond to 0.0, 0.098, 0.196, 0.487, 0.979, and 1.47 moles of LiCl per mole of polyol respectively.

The preparation of the plaques was carried out in a lab scale cup-foaming setup. Water (with a known amount of LiCl dissolved in it), and the polyol, were added to a cup and the mixture was stirred for 25 seconds at 2000 rpm with a 1" diameter stirrer. The TDI and the catalyst were then added and the mixture was stirred for another 15 seconds. The foam formation

was suppressed by forcing the foam to collapse by stirring. Just prior to gelation, the reacting mixture was quickly poured on Teflon sheets supported by steel plates and placed in a hot-press operating at 100 °C and 20,000 lb<sub>f</sub> for 1 hour. A picture-frame mold ca. 0.05” thick was utilized. At the end of 1 hour, the plaque was cut out from the picture-frame and allowed to cool at ambient conditions.

#### **4.3.2 Methods**

Small angle X-ray scattering (SAXS) was utilized to study the presence of microphase separation and to follow any trends in the interfacial behavior as a function of LiCl content. This was done using a Philips model PW1729 generator operating at 40 kV and 20 mA. A slit collimated (0.03 x 5 mm<sup>2</sup>) Kratky camera with nickel filtered CuK $\alpha$  radiation having a wavelength of 1.542 Å was used. The detector used was a Braun OED 50 position-sensitive platinum wire detector. The raw data was corrected for parasitic scattering and normalized using a Lupolen standard.

To investigate the local ordering of the hard segments at the 1-10 Å level, wide angle X-ray scattering (WAXS) was employed. WAXS experiments were carried out using a Phillips model PW1720 generator equipped with a Warhus camera. Pinhole collimated (ca. 0.02 in. diameter), nickel filtered CuK $\alpha$  radiation with a wavelength of 1.542 Å was used. Samples having a thickness of ca. 1.2 mm were exposed to the x-ray beam for 5 hrs, with a sample to film distance of 5.5 cm.

Transmission electron microscopy (TEM) was used to examine the urea particulates and their level of aggregation. The urea phase has a higher electron density as compared to the softer polyol phase and hence shows up as darker regions on the micrographs. Small samples were cut from the plaques and embedded in epoxy which was allowed to cure overnight at ambient conditions. The samples retained their original dimensions even after the surrounding epoxy had cured, suggesting that there was no chemical interaction between the epoxy and the samples. The samples were cut, both, parallel and perpendicular to the plane of the plaque and no directional dependence was observed via TEM (or AFM). A diamond knife was used to cryogenically microtome the samples into ultra-thin sections (ca. 80 nm) on a Reichert-Jung ultramicrotome Ultracut E equipped with a model FC-4D cryo-attachment operating at -90°C. The sections were then collected on 600 mesh copper grids using ethanol as a solvent. Micrographs were taken

using a Philips 420T scanning transmission electron microscope (STEM) operating at an accelerating voltage of 100 kV.

Tapping mode atomic force microscopy (*t*-AFM) experiments were carried out to study the micron size urea aggregates as well as to evaluate the presence, size, shape, and dispersion of nanoscopic level structures. The scans were performed on a Digital Instruments Scanning Probe Microscope employing a Nanoscope IIIa controller and Nanosensors TESP (Tapping Etched Silicon Probe) type single beam cantilevers. The cantilevers had nominal lengths of 125  $\mu\text{m}$ , with force constants in the range of  $35 \pm 7$  N/m, and were used at oscillation frequencies of ca. 295 kHz. The samples cryo-sectioned smooth for TEM were examined by AFM. The ‘height’ as well as the ‘phase’ images were collected, but since the samples were microtomed smooth, the height images were disregarded. In phase images obtained by *t*-AFM, a higher modulus material typically induces a higher phase offset and appears lighter as opposed to a softer phase which appears darker. Thus, for the polyurethanes imaged in this investigation, the urea rich regions appear lighter where as darker regions correspond to the softer polyol phase. For all the AFM images presented in this chapter, the free air oscillation amplitude was set at 60 nm, and the amplitude of the tip while striking the surface was maintained at ca. 58 % of this value.

Differential scanning calorimetry (DSC) experiments were conducted using a Seiko DSC 220C under a nitrogen purge and at a heating rate of 10  $^{\circ}\text{C}/\text{min}$ . The DSC curves were normalized to a 1 mg sample mass. DSC was carried out to observe any changes in the soft segment glass transition position and breadth on addition of LiCl.

Dynamic mechanical analysis (DMA) was carried out in the tensile mode using a Seiko model 210. The samples, with dimensions of approximately 15 x 4.5 x 1.2  $\text{mm}^3$ , were heated from  $-120$   $^{\circ}\text{C}$  to 250  $^{\circ}\text{C}$  at a rate of 2.0  $^{\circ}\text{C}/\text{min}$  from which the storage modulus and  $\tan\delta$  data were collected at a frequency of 1 Hz. The grip-to-grip distance was set at 10 mm.

Swelling experiments were carried out to determine the relative extent of cross-linking as a function of LiCl content. Samples weighing approximately 0.1 g were completely immersed in dimethyl-formamide (DMF) at ambient conditions and their equilibrium swelling level, which was achieved in ca. 10-12 hours, was recorded. To reinforce these results via a sol percentage analysis, these DMF swollen samples were then placed in an oven at 65 $^{\circ}\text{C}$  for 24 hours and weighed. The level of weight loss via this extraction process represents the sol fraction where as the extracted matrix represents the gel fraction.

#### 4.4 Results and Discussion

The results from the swelling and sol percentage analyses are presented in Table 4.1. Since LiCl is known to alter reactivity paths by lowering the effectiveness of the amine catalyst which catalyzes the ‘blow’ reaction,<sup>15</sup> it was considered essential to compare the quality of the network build-up in formulations with and without LiCl. From Table 4.1, it can be seen that the addition of LiCl did not cause drastic changes in the quality of the network, which is reflected by the equilibrium swelling level as well as the sol percentage of the different formulations. It is

<b>LiCl content (pphp)</b>	<b>Equilibrium Swelling Ratio</b> [DMF uptake (g) / sample weight (g)]	<b>Sol %</b>
0.0	1.8	3.5
0.1	1.8	3.3
0.2	1.5	2.8
0.5	1.6	1.3
1.0	1.6	1.9
1.5	2.2	3.4

**Table 4.1 – Equilibrium swelling ratio and sol % as a function of LiCl content**

observed that the equilibrium swelling content, measured as the weight of the solvent uptake normalized to the initial weight of the sample, for the samples incorporating LiCl is in the same range as that for the sample without the additive. In addition, the sol percentage was found to be 3.5 % for the sample with no LiCl, and was found to be always lower than this value for the formulations containing LiCl. Thus it can be concluded that the incorporation of LiCl did not inhibit the formation of a covalent network; in fact, these data indicate that the addition of LiCl led to a network which had a cross-link density somewhat similar to the cross-link density of the same formulation without LiCl.

The SAXS profiles for the plaques are shown in Figure 4.1 where the normalized scattered intensity is plotted as a function of the scattering vector ‘s’. The scattering vector is defined as  $s = (2/\lambda)\sin(\theta/2)$  where  $\lambda$  is the wavelength of the x-ray source and  $\theta$  is the radial scattering angle. Though SAXS does not provide a direct image of the morphology of the

material, structural information at length scales ranging from ca. 10 Å to ca. 500 Å can be indirectly obtained from the scattering curve. In particular, this study focuses on three regions of the scattering curve. The low ‘s’ region ( $s < 0.005 \text{ \AA}^{-1}$ ) has been utilized to evaluate the presence/absence of the urea aggregates discussed previously, since these large aggregates would have a significant contribution to the scattering intensity in this region. The intermediate ‘s’

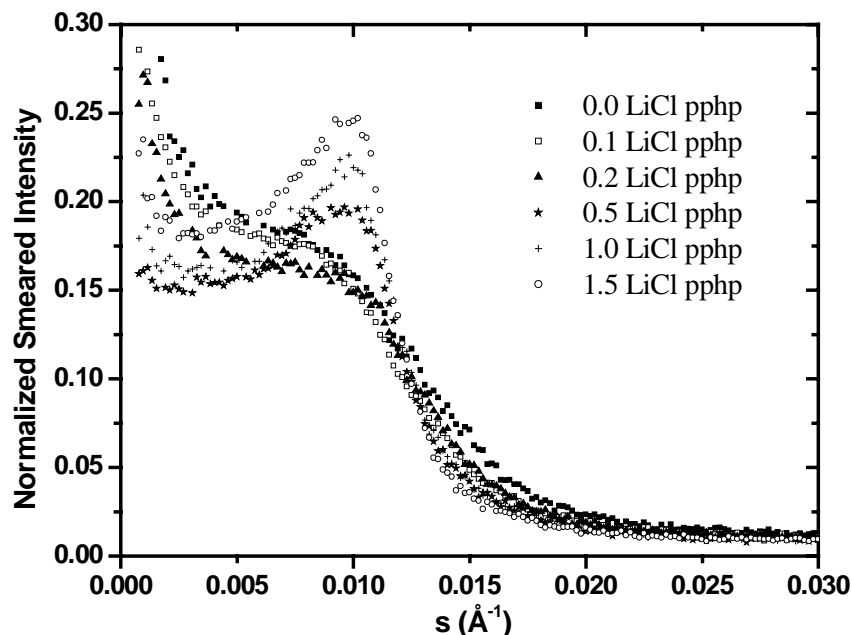


**Figure 4.1** Small angle x-ray scattering profiles as a function of LiCl content.

values ( $s \sim 0.01 \text{ \AA}^{-1}$ ) are used to estimate the average interdomain spacing, which for flexible polyurethane foam formulations is known to be of the order of 80-120 Å.<sup>5</sup> Finally, the angular dependence of the tail region ( $s > 0.02 \text{ \AA}^{-1}$ ) is dependent on the thickness of the boundary between the hard and the soft phase and is thus utilized to analyze the effect of LiCl on the interfacial behavior.<sup>5</sup>

It can be observed from Figure 4.1 that addition of LiCl at 0.1, 0.2, and 0.5 pphp led to a systematic drop in the scattering intensity at low ‘s’ values suggesting that LiCl suppressed the formation of the large urea rich aggregates. This observation was also supported by the TEM and *t*-AFM micrographs (discussed later) and by noting that the plaque without LiCl was opaque and the plaques became clearer or more transparent as the LiCl content was increased. However, the formulations incorporating 1.0 and 1.5 LiCl pphp did not follow this trend and displayed a relative increase in scattering intensity at small ‘s’ values as compared to the plaque with 0.5

LiCl pphp. This could be due to the fact that these formulations had some micro-voids present in them which could contribute to the scattering intensity at lower angles. (The presence of the micro-voids could be due to the fact that for formulations with high LiCl content, the blow reaction takes a longer time to proceed and thus some of the carbon dioxide induced voids during the later stages of plaque preparation). At an 's' value of ca.  $0.01 \text{ \AA}^{-1}$  a first order interference was observed for all formulations, the position of which did not change on varying the LiCl content. This suggested that all the systems studied displayed some level of microphase separation that possessed an interdomain spacing of ca.  $100 \text{ \AA}$ , in conformity with earlier results obtained for flexible foam formulations.<sup>5</sup> This first order interference peak appeared in the form of a weak shoulder for the formulation containing no LiCl and transformed into a sharper shoulder for intermediate LiCl contents and was observed as a peak at high LiCl contents. This observation can be explained as follows. In the formulation with no LiCl, since the urea microdomains reside both in the urea rich aggregates as well as in the polyol phase, the distribution of the interdomain spacing would be wider and hence the first order interference appears as a weak shoulder. On the other hand, in formulations containing LiCl, since the urea rich aggregates are not formed, this leads to a more uniform distribution of the urea microdomains and hence a sharper shoulder or peak is observed. This observation will be further supported in this report by the TEM and AFM results. Finally, a SAXS interfacial analysis on the tail region using Bonart's method described in reference 16 led to an interfacial thickness parameter in the range of  $5.5 - 8.0 \text{ \AA}$  for all the foams studied, with no systematic trend observed. This indicated that there existed a similar extent of phase mixing *at the interface* of the soft and hard segments in all the formulations. This observation, along with the fact that the interdomain spacing remained unchanged with LiCl content, indirectly indicated that the molecular weight distribution of the hard segments remained almost constant with LiCl content.

Over the years, TEM has proven to be a useful technique to analyze the presence of the large urea rich aggregates which possess higher electron densities and thus show up as darker regions on the micrographs.<sup>3,4,5</sup> However, since TEM (and AFM) image cross-sectional areas rather than a three-dimensional volume, these techniques are somewhat inadequate in examining the morphology of a material. Figure 4.2a, corresponding to the plaque with no LiCl, showed the presence of precipitates which are of the order of  $0.2 - 0.5 \text{ \mu m}$  in size. It can be observed from Figures 4.2b to 4.2f that addition of LiCl leads to a reduction in the urea aggregation level, as

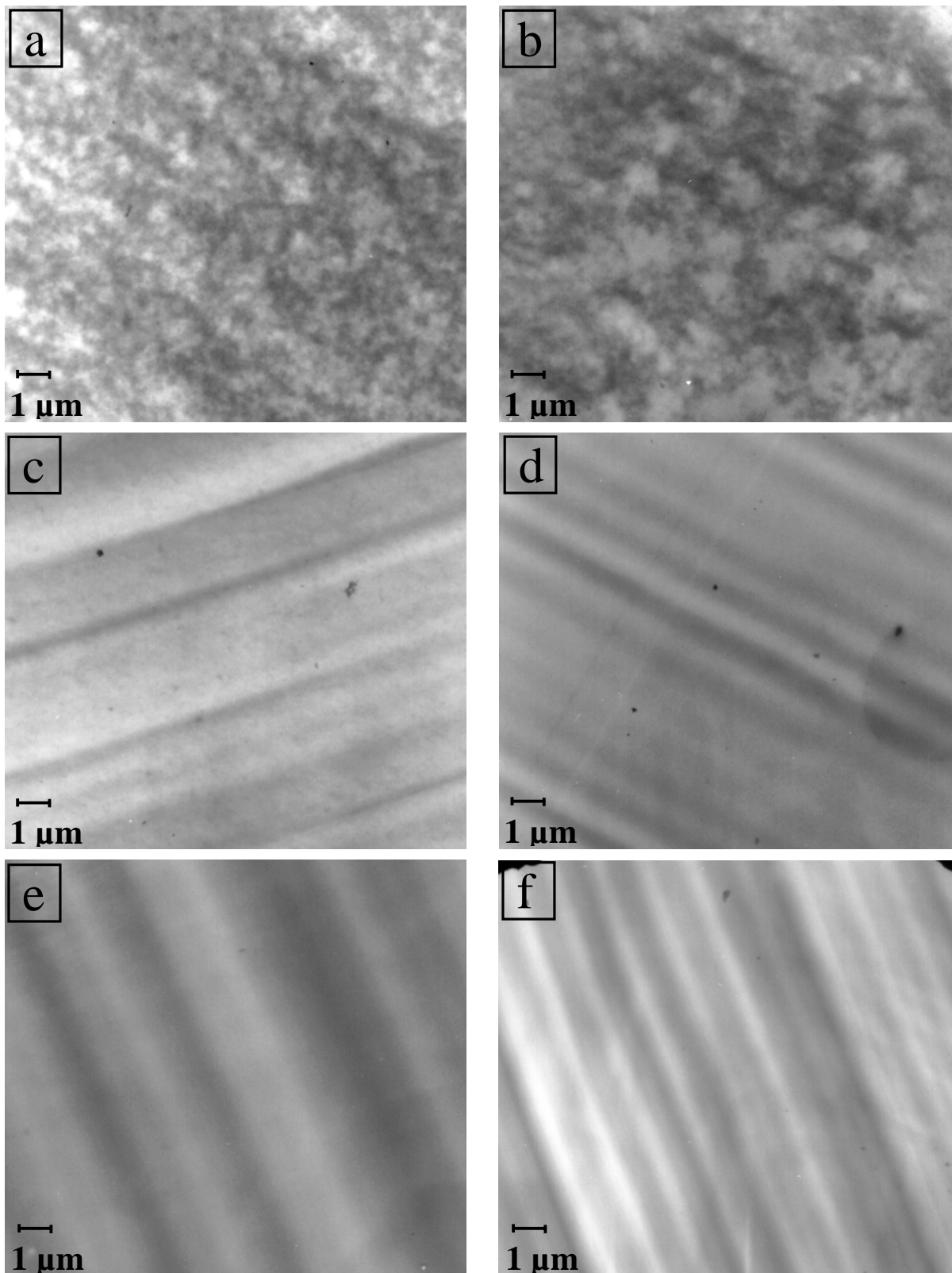


**Figure 4.2** Transmission electron micrographs of plaques with varying LiCl content: a) 0.0 LiCl pphp, b) 0.1 LiCl pphp, c) 0.2 LiCl pphp, d) 0.5 LiCl pphp, e) 1.0 LiCl pphp, and f) 1.5 LiCl pphp.

indicated earlier by SAXS. It can be noted from Figure 4.2b that addition of LiCl even at a small amount of 0.1 LiCl pphp leads to a noticeable reduction in the urea rich aggregates; both in terms of the number of aggregates formed, as well as the size of each aggregate. This decrease in urea aggregation with increasing LiCl content was found to be systematic. At 0.2 LiCl pphp, the aggregates are observed to be considerably smaller and are at best estimated to be less than 0.1  $\mu\text{m}$  in size. The reduction in the size of aggregates also clearly reduces the *macro* level connectivity – aggregates which appeared to have physical associations with each other at 0.0 and 0.1 LiCl pphp are observed to be comparatively isolated at 0.2 LiCl pphp. At this point, a drawback in using TEM as a technique to examine *macro* level connectivity is recognized. The *macro* aggregate connectivity observed via TEM images is limited to the cross-section that TEM examines, i.e., a quantification of the extent of *macro* connectivity of the urea phase at the three-dimensional level cannot be made via TEM. A further increase in LiCl content leads to a further reduction in the urea aggregation and micrographs corresponding to 0.5, 1.0 and 1.5 LiCl pphp do not show any aggregation behavior, or, the aggregates are smaller than what can be examined by TEM. It also needs to be pointed out that the parallel sets of lines observed in Figures 4.2c-4.2f are ‘chatter marks’ introduced due to the microtoming process and are by no means related to the morphology of the plaques.

WAXS patterns for the plaques with 0.0 LiCl pphp and 1.5 LiCl pphp are shown in Figures 4.3a and 4.3b. A weak but distinct diffraction peak corresponding to a 4.7  $\text{\AA}$  spacing is

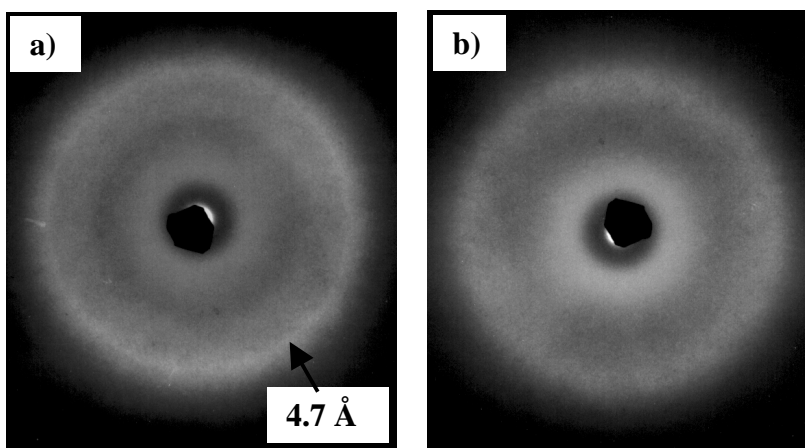


**Figure 4.3 Wide angle x-ray scattering patterns for plaques: a) 0.0 LiCl pphp and b) 1.5 LiCl pphp.**

observed in the 0.0 LiCl pphp plaque where as this peak is found to be absent in the 1.5 LiCl pphp plaque. Plaques with intermediate LiCl content show a loss in the peak intensity as LiCl

content is increased and are thus not presented here. Though an exact understanding of the source of this reflection is not completely identified, it has been postulated to be due to the existence of hydrogen bonding and indicates that the hard domains possess internal order of a somewhat paracrystalline nature.<sup>5,17</sup> The patterns thus suggest that addition of LiCl not only leads to a reduction in order at the urea aggregate level, but also alters the *micro*-connectivity or the regularity in packing order between the hard segments themselves.

In recent work by Kaushiva et. al.<sup>4</sup> and in Chapter 3 of this dissertation, *t*-AFM was demonstrated as an effective technique to study flexible polyurethane foam morphology. In that study, it was established that phase images obtained via *t*-AFM were comparable to the images obtained by TEM at the same magnification. This observation was reconfirmed in the present study by juxtaposing the *t*-AFM and TEM images of the sample without LiCl (Figure 4.4). *It needs to be noted that the contrast of the AFM phase images in Figures 4.4 and 4.5 has been deliberately inverted so that the harder material has a lower phase offset and appears darker. This was done so that a visual comparison of the AFM phase images vs. TEM images could be made. However, all other AFM images in this chapter are presented in the conventional manner whereby the harder material has a higher offset and appears lighter.* Furthermore, it can be observed from Figure 4.5, that AFM phase-imaging was able to distinguish the hard and soft phases at 1.0 LiCl pphp, while TEM was ineffective in this case. Therefore, the advantage of AFM, for the materials investigated in this study, lies in the fact that AFM has the power to more easily probe a much wider range of length scales as compared to TEM; and thus, in addition, can be used to give valuable information even at the microdomain level. Figure 4.6 presents 500 x 500 nm<sup>2</sup> *t*-AFM phase images for the six samples studied. It can be observed that *t*-AFM had the capability to resolve morphological features even at such high magnifications. Figure 4.6a shows that in the plaque with no LiCl, urea rich regions of the order of 50-100 nm in size exist. In the same image, polyol rich areas of the order of 50-100 nm can also be observed. On addition of 0.1 LiCl pphp, the urea rich regions are found to be reduced to ca. 25-50 nm in size. On increasing LiCl content to even higher levels, a further reduction in the size of the urea rich regions is observed and at 1.0 and 1.5 LiCl pphp these urea rich regions are believed to be close to the microdomain size. Also at these LiCl contents, the polyol rich areas which were observed in the plaque with no LiCl are found to be absent. These data again suggest that incorporation of LiCl breaks up larger urea rich phases and disperses them more uniformly and in a more continuous

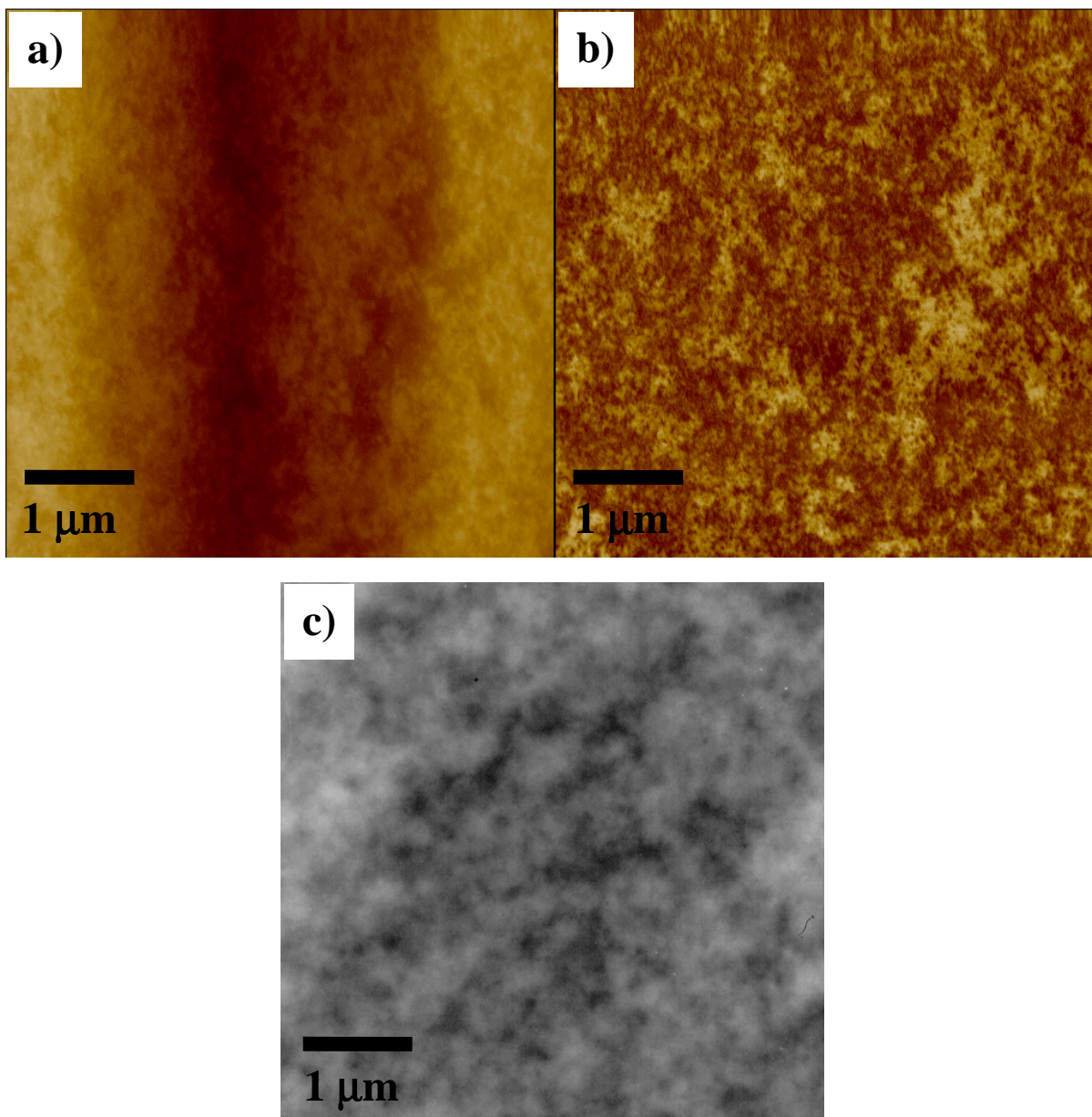


**Figure 4.4** Comparison of t-AFM and TEM images for the plaque containing 0.0 LiCl pphp. a) t-AFM height image b) t-AFM phase image c) TEM image. *A comparison of the AFM height image with the corresponding phase image suggests that the phase image is not influenced.*

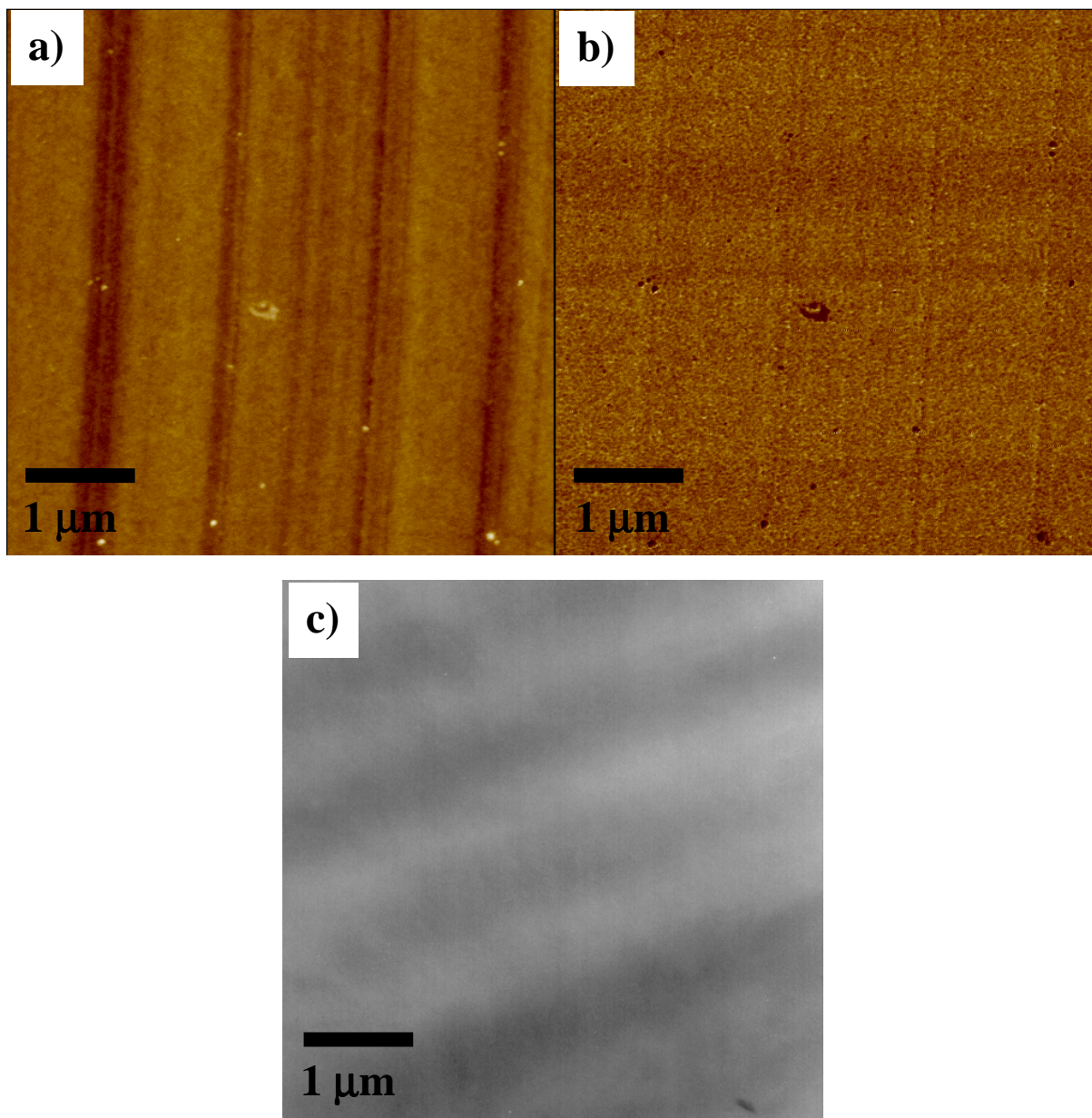


**Figure 4.5 Comparison of t-AFM and TEM images for the plaque containing 1.0 LiCl pphp. a) t-AFM height image b) t-AFM phase image c) TEM image.**

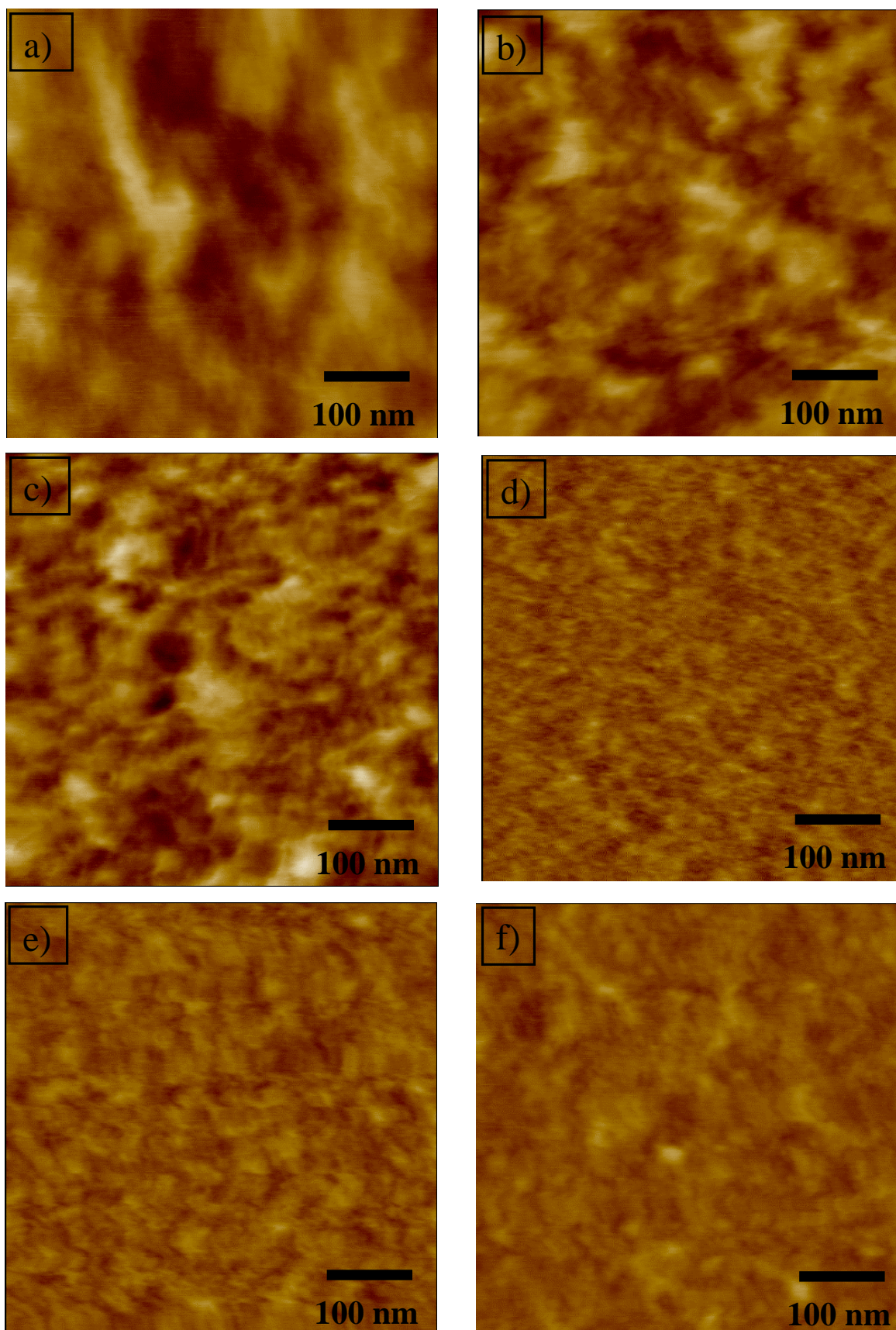


**Figure 4.6 Atomic force microscopy phase images for samples with varying LiCl content: a) 0.0 LiCl pphp, b) 0.1 LiCl pphp, c) 0.2 LiCl pphp, d) 0.5 LiCl pphp, e) 1.0 LiCl pphp, and f) 1.5 LiCl pphp.**

fashion in the polyol phase. Clearly, the samples with 0.0 LiCl pphp and 1.5 LiCl pphp possess greatly varying connectivity levels at the microdomain level, and this is expected to affect the mechanical performance of the polymer. It also needs to be pointed out that the AFM and TEM images presented in this chapter are repeatable. This was confirmed by examining several regions of the samples by the two techniques.

DSC was utilized to ascertain the effect of adding LiCl on the soft segment glass transition and phase separation characteristics. It was observed from the DSC scans (Figure 4.7) that the breadth and position of this  $T_g$  remained relatively constant for all the six samples

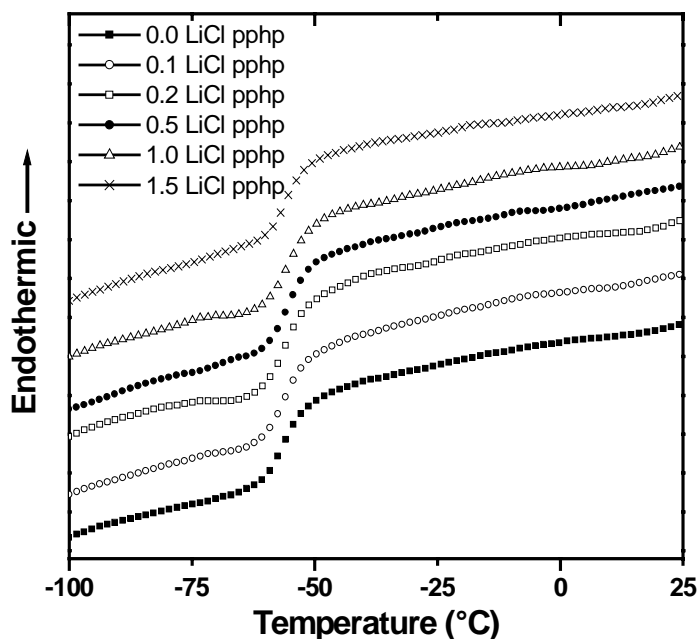


**Figure 4.7 Soft segment glass transition observed via DSC as a function of LiCl content.**

examined. This implied that even though the urea phase existed in strikingly different structures, the mobility of the soft phase in all the six samples remained relatively unchanged. Further support of this observation was gained via DMA by which the temperature position of the  $Tan\delta$  peak, as well as its breadth, were also noted to be very similar for all the samples (data not presented).

#### 4.5 Conclusions

This study has utilized LiCl as an additive to alter and thus gain insight into urea phase connectivity in molded flexible polyurethane foam formulations. The characterization techniques

of SAXS, WAXS, TEM, AFM, DSC, and DMA were applied to characterize urea phase connectivity which was found to occur over different length scales. DSC and DMA were used to ascertain that formulations with and without LiCl possessed similar soft segment glass transition breadths and positions, thus indicating that the soft segment mobility was unaffected on addition of LiCl. SAXS was used to show that addition of LiCl to the formulation did not prevent the formation of urea microdomains commonly observed in flexible polyurethane foam formulations. The regularity in hard segment packing, or the *micro*-connectivity of the urea phase; which was observed using WAXS, was noted to be disrupted on addition of LiCl. SAXS, TEM, and *t*-AFM were collectively used to probe the presence, size, as well as the physical associations of urea rich aggregates. These techniques thus provided information on the *macro* level connectivity of the urea phase, which was found to be lost on addition of LiCl. *t*-AFM was shown to be useful to observe the dispersion of the urea microdomains in the polyol matrix, and thus gave insight into the effect of LiCl on urea microdomain level connectivity.

Previous studies have attributed the observed increase in the modulus of flexible polyurethane foams on increasing the hard segment content to the enhanced filler-like effect the urea hard phase causes, and also to the increased number of physical cross-linking points in the foam. However, the significance of urea phase connectivity, and the opportunity it presents in altering the physical properties of the foam has not been clearly addressed. This work has therefore taken a step towards understanding the level of urea phase connectivity which might be present in molded flexible foam materials. The results of a more comprehensive study, where the influence of urea phase connectivity on the thermal and viscoelastic properties of *actual* flexible foam formulations and their plaque counterparts has been studied, are presented in Chapter 6.

## 4.6 References

- 
1. Hepburn, C. Polyurethane Elastomers, 2<sup>nd</sup> ed.; Elsevier Applied Science: London, 1991.
  2. Chemical and Engineering News: May 29, 2000, 78, 42.
  3. Herrington, R.; Hock, K. Flexible polyurethane foams, 2<sup>nd</sup> ed.; Dow Chemical Co.: Midland, MI, 1998.
  4. Kaushiva, B.D.; McCartney, S.R.; Rossmly, G.R.; Wilkes, G.L. Polymer 2000, 41, 285.
  5. Armistead, J.P.; Wilkes, G.L.; Turner, R.B. J Appl Polym Sci 1988, 35, 601.
  6. Moreland, J.C.; Wilkes, G.L.; Turner, R.B. J Appl Polym Sci 1994, 52, 549.
  7. Ade, H.; Smith, A.P.; Cameron, S.; Cieslinski, R.; Mitchell, G.; Hsiao, B.; Rightor, E. Polymer 1995, 36, 1843.

- 
8. Kaushiva, B.D.; Dounis, D.V., Wilkes, G.L. *J Appl Polym Sci* 2000, 78, 766.
  9. Kaushiva, B.D.; Wilkes, G.L. *J Appl Polym Sci* 2000, 77, 202.
  10. Kaushiva, B.D.; Wilkes, G.L. *Polymer Commun* 2000, 41, 6981.
  11. Moreland, J.C.; Wilkes, G.L.; Turner, R.B.; Rightor, E.G. *J Appl Polym Sci* 1994, 52, 1459.
  12. Gao, T. *Gaofenzi Tongxun* 1984, 1, 69.
  13. van Heumen, J.D.; Stevens, J.R. *Macromolecules* 1995, 28, 4268.
  14. Wang, H.L., Kao, H.M., Digar, M; Wen, T.C. *Macromolecules* 2001, 34, 529.
  15. Priester, R.D. of Dow Chemical Co., personal communication.
  16. Tyagi, D.; McGrath, J.E.; Wilkes, G.L. *Polym Eng and Sci* 1986, 26, 1371.
  17. Dounis, D.V.; Wilkes, G.L. *Polymer* 1997, 38, 2819.